ISSN 1028-3358, Doklady Physics, 2012, Vol. 57, No. 2, pp. 92–95. © Pleiades Publishing, Ltd., 2012.
Original Russian Text © E.A. Podolskaya, A.M. Krivtsov, A.Yu. Panchenko, P.V. Tkachev, 2012, published in Doklady Akademii Nauk, 2012, Vol. 442, No. 6, pp. 755–758.

MECHANICS

Stability of Ideal Infinite Two-Dimensional Crystal Lattice

E. A. Podolskaya, A. M. Krivtsov, A. Yu. Panchenko, and P. V. Tkachev

Presented by Academician N.F. Morozov October 17, 2011

Received November 7, 2011

DOI: 10.1134/S1028335812020115

Currently, in connection with the development of nanotechnologies, it is necessary to evaluate the strength properties of bodies containing a finite number of atomic layers. Such objects are often defect-free, and, as a consequence, their strength is close to theoretical or ideal strength. McMillan [1] considered the question on the experimental measurement of the ideal strength, as the critical stress is called. When determining this quantity, it is necessary to verify the stability of the deformed body relative to any additional small deviation for each stress or strain increment.

Born established that the crystal lattice is stable with respect to small uniform deformations if the elastic energy density calculated for equilibrium is the positive-definite quadratic form [2]. It was shown that close-packed FCC and HCP structures are stable in small for any pair central force interparticle interactions [3]. However, it was shown that problems appear when trying to apply the Born criterion in the case of finite deformations [4].

Recently, a series of independent investigations into the stability [5, 6] of a new nanomaterial graphene (one graphite layer) under large deformations was performed with the use of interaction potentials and with thermal atomic vibrations and the influence of boundary conditions neglected [7, 8]. Frequencies of elastic waves were required to be real as the stability criterion. The investigation into graphene stability is a rather complex problem, which is associated both with the lattice geometry and with the applied interaction potentials. We consider a simpler object, which allows us to acquire an analytical solution.

Institute of Problems in Mechanical Engineering, Russian Academy of Sciences, Vasil'evskii Ostrov, Bol'shoi pr. 61, St. Petersburg, 199178 Russia
e-mail: katepodolskaya@gmail.com

The aim of this work is to investigate the stability of the ideal two-dimensional triangular crystal lattice, which is a single atomic layer in the FCC and HCP structures. The interparticle interaction in this lattice is described using the pair central force interaction. This is a convenient and simple model for construction of the theory, analytical calculations, and computational experiments.

This work continues investigation [9], where a part of the stability region of the two-dimensional triangular lattice is presented without shear. The initial problem was to establish the physical sense of the stability region found analytically in [10] and to verify the acquired results using the numerical experiment. However, detailed investigation into the problem showed the existence of additional stability regions associated with the structural transition in the material.

We apply direct tensor calculus [11]. As the interaction law, we use Morse $\Pi(r)$ and Lennard-Jones $\Pi_{LJ}(r)$ potentials:

$$\Pi(r) = D\left[\exp\left(-2\theta\left(\frac{r}{a}-1\right)\right) - 2\exp\left(-\theta\left(\frac{r}{a}-1\right)\right)\right],$$
$$\Pi_{LJ}(r) = D\left[\left(\frac{a}{r}\right)^{12} - 2\left(\frac{a}{r}\right)^{6}\right]. \quad (1)$$

Parameter D is responsible for the potential well depth, and parameter θ is responsible for its width. Near the equilibrium position at $\theta = 6$, Morse potential is equivalent to Lennard-Jones potential with the same values of the potential well depth and equilibrium distance a [12]. An important distinction of Morse potential from Lennard-Jones potential is that during the compression of the material to the point ($r = 0$), the interaction force remains finite, e.g. at $\theta = 6$, the repulsion force is of the order of $10^6 D/a$. This allows us to perform the molecular-dynamic simulation under strong compression. In addition, rapid attenuation of exponents allows us to take into account the smaller number of coordination spheres.

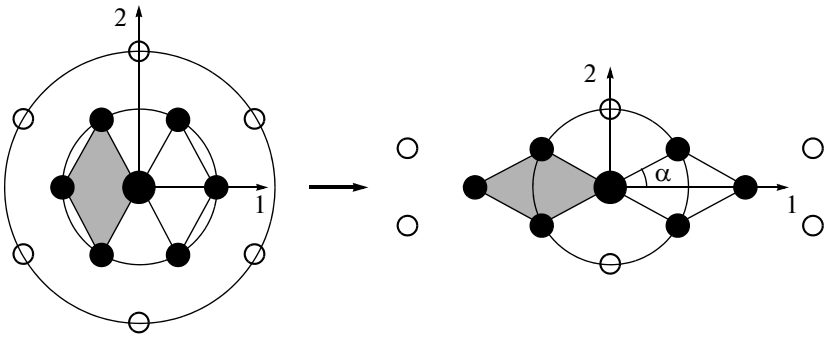

Fig. 1. Transition from vertical to horizontal orientation of the triangular lattice. Digits denote the coordinate axes. The unit cell is gray, the reference atom is marked by a circle, the atoms of the first coordination sphere are marked by circles of a smaller radius, and the atoms of the second coordination sphere are marked by empty circles.

To describe the material, the equation of motion of a continuous medium in the Piola form is used [11]:

$$\rho\ddot{\mathbf{u}} = \overset{\circ}{\nabla} \cdot \mathrm{P}, \tag{2}$$

where $\mathbf{u}$ is the displacement vector, $\mathbf{P}$ is the Piola stress tensor, and $\overset{\circ}{\nabla}$ is the Hamiltonian operator in the reference configuration.

We further use the first variation of Eq. (2) near the deformed state of the crystal lattice. As a result of transformations, we derive the equation

$$\ddot{\mathbf{v}} = {}^4\mathbf{Q} \cdots (\nabla\nabla\mathbf{v}), \tag{3}$$

where $\mathbf{v} = \delta\mathbf{u}$ is the first variation of the displacement vector, ∇ is the Hamiltonian operator in the actual configuration, and ${}^4\mathbf{Q}$ is the fourth-rank acoustic tensor depending on the first and second derivatives of the interaction potential (forces in bonds and bond rigidity) as well as on the geometry of the particle surroundings [11, 12]. The solution of Eq. (3) in wave form is

$$\mathbf{v} = \mathbf{v}_0 e^{i\omega t} e^{i\mathbf{KR}}, \tag{4}$$

where $\mathbf{K}$ is the wave vector and ω is the frequency. Solution (4) describes the wave if frequency ω is also real for any real wave vector $\mathbf{K}$, i.e., $\omega^2 > 0$ (the dynamic stability criterion). The static stability criterion is the positivity of the Young modulae and shear modulae [11], which are determined in the actual (deformed) configuration.

Substituting (4) in (3), we acquire the set of linear uniform equations $(\mathbf{D} - \omega^2\mathbf{E}) \cdot \mathbf{v}_0 = 0$, which has a nontrivial solution at its zero determinant. Tensor $\mathbf{D}$ is determined by formula $\mathbf{D} = {}^4\mathbf{Q} \cdot\cdot \mathbf{KK}$, where $\mathbf{E}$ is the identity tensor.

For the two-dimensional lattice, the stability conditions are written in the form

$$I_1(\mathbf{D}) > 0, \quad I_2(\mathbf{D}) > 0, \quad 2I_1(\mathbf{D}^2) \geq I_1^{\,2}(\mathbf{D}), \tag{5}$$

where I_1 and I_2 are the main invariants of tensor $\mathbf{D}$. Inequalities (5) should hold at any $\mathbf{K}$. The last inequality is fulfilled identically for the two-dimensional case. This means that the quadrate of frequency passes through zero upon changing the sign; consequently, the dynamic stability criterion coincides with the static one in this case.

Figure 1 depicts a characteristic part of the triangular lattice before and after deformation. We marked the axes along which deformation is implemented. Before the deformation, angle $\alpha = 60°$. Let us introduce an orthonormal basis so that vector $\mathbf{e}_1$ is codirectional with axis 1, and vector $\mathbf{e}_2$ is codirectional with axis 2.

When considering large deformations, we should take into account more than one coordination sphere, for example, for the correct description of the transition from the vertical lattice orientation to the horizontal one (Fig. 1), which results into the same lattice turned by 90°. In Fig. 1, the unit cell is gray, the reference atom is marked by a circle, the atoms of the first coordination sphere are marked by circles of a smaller radius, and the atoms of the second coordination sphere are marked by empty circles. We can see that the atoms from the second coordination sphere are involved as nearest neighbors of the reference atom in the reoriented lattice. If we exclude the atoms of the second sphere, we will obtain an evidently unstable configuration instead of the second equilibrium position. Additional investigation showed that consideration of the next coordination spheres does not noticeably affect the stability region.

In the case of deformation without shear (Fig. 1), conditions (5) take the form

$$Q_{11} > 0, \quad Q_{12} > 0, \quad Q_{21} > 0, \quad Q_{22} > 0, \tag{6}$$

$$B > -\sqrt{AC}, \tag{7}$$

where $A = Q_{11}Q_{21}$, $C = Q_{12}Q_{22}$, $2B = Q_{11}Q_{22} + Q_{12}Q_{21} - 4Q_{44}^2$, Q_{ij} are the components of tensor ${}^4\mathbf{Q}$. In addition, Q_{ij} $(i, j = 1, 2)$ are the quadrates of velocities of wave propagation. Condition (6) is necessary since all

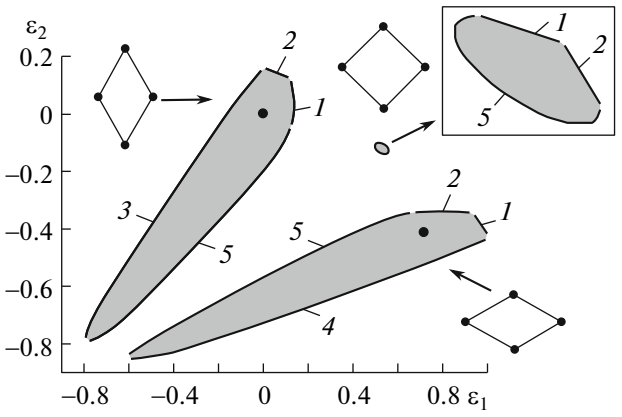

Fig. 2. Stability regions of the triangular lattice in deformation space ε_1, ε_2 without shear. The interaction is described by Morse potential. The boundaries of the regions are determined by equations: (*1*) $Q_{11} = 0$, (*2*) $Q_{22} = 0$, (*3*) $Q_{21} = 0$, (*4*) $Q_{12} = 0$, and (*5*) $B = -\sqrt{AC}$, where $A = Q_{11}Q_{21}$, $C = Q_{12}Q_{22}$, $2B = Q_{11}Q_{22} + Q_{12}Q_{21} - 4Q_{44}^2$, and Q_{ij} are the components of the acoustic tensor ${}^4\mathbf{Q}$.

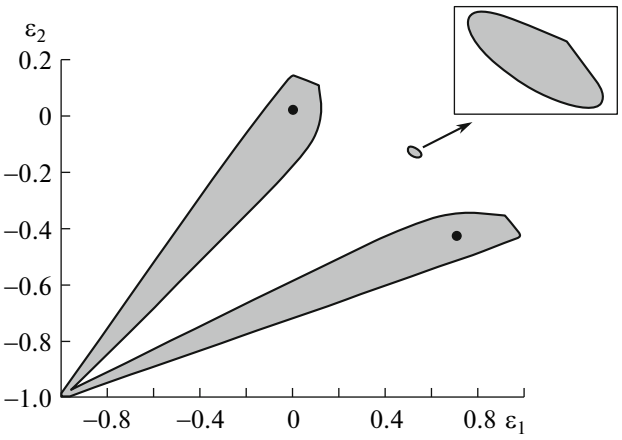

Fig. 3. Stability regions of the triangular lattice in deformation space ε_1, ε_2 without shear. The interaction is described by Lennard-Jones potential.

velocities of wave propagation are real in the case of stability [11].

In Fig. 2, the stability regions of the two-dimensional triangular lattice are gray, ε_1 and ε_2 are the linear parts of the Cauchy–Green deformation tensor, and the interaction is performed by means of Morse potential (1) with parameter $\theta = 6$. Condition (7), which supplements conditions (6), allows us to distinguish three stability regions, which correspond to the horizontal and vertical lattice orientations and also to the intermediate square configuration.

The form and number of the regions depend on the selection of the interaction potential. As parameter θ decreases, the intermediate region disappears. An independent investigation showed that the use of Lennard-Jones potential provides stability of the material during its hydrostatic compression, i.e., during its deformation along line $\varepsilon_1 = \varepsilon_2$, right up to deformations arbitrarily close to point $\varepsilon_1 = \varepsilon_2 = -1$ (Fig. 3).

Let us show that the dynamic stability criterion coincides with the static one. For this purpose, let us calculate the Young modulae and shear modulae for each deformed configuration using representation [12] for Cauchy stress tensor:

$$\boldsymbol{\sigma} = \frac{1}{2V}\sum_k \mathbf{A}_k\mathbf{F}_k,$$

where $V = \frac{\sqrt{3}}{2}(\varepsilon_1 + 1)(\varepsilon_2 + 1)$ is the unit cell volume, $\mathbf{A}_k$ are the radius-vectors of the particles relative to the reference atom (it is in the hexagon center in Fig. 1), $\mathbf{F}_k$ are the vectors of interaction forces, and $F_k = -\Pi'(A_k)$.

The positivity requirement for the Young modulae E and shear modulae G leads to the result coinciding with that presented in Fig. 2, namely, the Young modulae change the sign at boundaries *1*, *2*, and *5*; the shear modulae change the sign at boundaries *3* and *4*; and all the modulae are positive and the deformed state is stable in gray zones. The stability loss during hydrostatic compression is associated with a sign change of the shear modulus, which agrees with the results of calculations for the FCC lattice [13].

To verify the obtained results, we use the particle dynamics method. The simulation technique is described in [12]. For a series of deformed configurations, we perform the following computational experiment. As the initial condition, we construct a triangular lattice in the deformed state with periodic boundary conditions. The interparticle interaction is described by means of Morse potential (1). The initial kinetic energy of the particles does not exceed $0.0002D$. The system evolution is described by the solution of the Cauchy problem for the set of ordinary differential equations

$$m\ddot{\mathbf{r}}_k = \sum_{n=1}^{N} F(|\mathbf{r}_k - \mathbf{r}_n|)\frac{\mathbf{r}_k - \mathbf{r}_n}{|\mathbf{r}_k - \mathbf{r}_n|}, \quad k = 1,2,\ldots,N, \qquad (8)$$

where N is the number of particles, m is the particle mass, and $\mathbf{r}_k$ is the radius-vector of the kth particle. If we further observe oscillations of the kinetic energy around a certain value not exceeding $0.0002D$ limited by amplitude, we conclude that this configuration is stable. If we observe a sudden growth of the kinetic energy, the deformed configuration is considered unstable. The regions obtained as a result of the

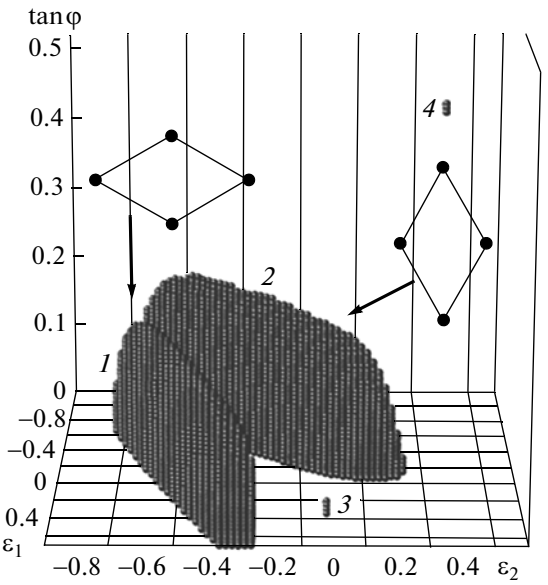

Fig. 4. Stability regions of the triangular lattice in deformation space ε_1, ε_2, φ. The interaction is described by Morse potential. Stability regions correspond to (*1*) horizontal lattice orientation, (*2*) vertical lattice orientation, (*3*) square configuration at $\varphi \approx 0$, and (*4*) square configuration at $\varphi \approx 26°$.

molecular-dynamic simulation coincide with those presented in Fig. 2 accurate to the exactness of computer calculations. The elapsed time for the construction of stability regions was incommensurably larger than in the analytical approach.

We also solved a similar problem for deforming the triangular lattice allowing for the shear. We found two main and two intermediate regions in the three-dimensional space of deformations ε_1, ε_2, φ, which corresponded to two lattice orientations and square configurations at shear angle $\varphi \approx 0$ and $\varphi \approx 26°$. These regions are symmetric relative to plane $\varphi = 0$ (Fig. 4).

Thus, the stability of the two-dimensional triangular lattice under finite deformation is investigated. The structural transition from the vertical lattice orientation to the horizontal one is described (Fig. 2). The problem is solved analytically for the case of biaxial deformation. The boundaries of the stability regions found are explained both in terms of coefficients of wave equation (3) and using the Young modulus and shear modulus, which cannot be negative in the actual material. When using Lennard-Jones potential, the material does not lose stability under arbitrarily large hydrostatic compression. The application of Morse potential in the same conditions allows us to describe the stability loss and to show that instability is associated with variation in the sign of the shear modulus. The results of analytical calculations are proved by the molecular-dynamic simulation.

REFERENCES

1. A. Yu. Ishlinskii, *Atomistics of Fracture: Selected Articles 1983–1985* (Mir, Moscow, 1987) [in Russian].
2. M. Born and K. Huang, *Dynamical Theory of Crystal Lattices* (Clarendon, Oxford, 1954).
3. D. C. Wallace and J. L. Patrick, Phys. Rev. **137** (1A), 152 (1965).
4. J. Wang, J. Li, S. Yip, S. Phillpot, and D. Wolf, Phys. Rev. **52** (17B), 12627 (1995).
5. P. E. Tovstik and T. P. Tovstik, Vestn. SPbGU, issue 3, (2009), p. 1.
6. S. V. Dmitriev, Yu. A. Baimova, A. V. Savin, and Yu. S. Kivshar', Pis'ma Zh. Eksp. Teor. Fiz. **93** (10), 632 (2011).
7. I. E. Berinskii, E. A. Ivanova, and A. M. Krivtsov, Izv. Ross. Akad. Nauk, Mekh. Tverd. Tela, No. 5, 6 (2007).
8. A. V. Savin, Yu. S. Kivshar, and B. Hu, Phys. Rev. **82**, 195422 (2010).
9. P. V. Tkachev and A. M. Krivtsov, *XXXIII Science Week of SPbGPU: Mater. Int. Sci.-Practical Conf.* (Politekhn. Univ., St. Petersburg, 2004), Chap. V, p. 4 [in Russian].
10. E. A. Podolskaya, P. V. Tkachev, and A. M. Krivtsov, *XXXIX Science Week of SPbGPU: Mater. Int. Sci.-Practical Conf.* (Politekhn. Univ., St. Petersburg, 2010), Chap. V, p. 111 [in Russian].
11. A. I. Lurie, *Nonlinear Theory of Elasticity* (Nauka, Moscow, 1980) [in Russian].
12. A. M. Krivtsov, *Deformation and Fracture of Solids with Microstructure* (Fizmatlit, Moscow, 2007) [in Russian].
13. F. Milstein and D. Rasky, Phys. Rev. **54** (10), 7016 (1996).

Translated by N. Korovin